Accepted Manuscript

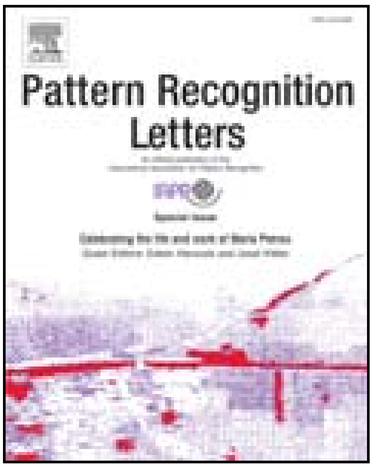

A Multilevel Color Image Thresholding Scheme based on Minimum Cross Entropy and Differential Evolution

Soham Sarkar , Swagatam Das , Sheli Sinha Chaudhuri

PII: S0167-8655(14)00359-6
DOI: 10.1016/j.patrec.2014.11.009
Reference: PATREC 6129

To appear in: *Pattern Recognition Letters*

Received date: 27 May 2014
Accepted date: 26 November 2014

Research Highlights

- A new multi-level thresholding approach is proposed for colour images.
- The minimum cross-entropy approach is extended to colour images.
- Simple evolutionary search is used to solve the underlying optimization problem.
- The proposed method is validated by using the Berkley Segmentation Data Sets.

A Multilevel Color Image Thresholding Scheme based on Minimum Cross Entropy and Differential Evolution

Soham Sarkar[a], Swagatam Das[b],* and Sheli Sinha Chaudhuri[c]

[a] *Dept. of Electronics and Communication Engineering, RCC Institute of Information Technology, Kolkata 700015, India*
[b]*Electronics and Communication Sciences Unit, Indian Statistical Institute, Kolkata 700 108, India*
[c]*Dept. of Electronics and Telecommunication Engineering, Jadavpur University, Kolkata 700032, India*

Abstract

We propose a novel multi-level thresholding method for unsupervised separation between objects and background from a natural color image using the concept of the Minimum Cross Entropy (MCE). MCE based thresholding techniques are widely popular for segmenting grayscale images. Color image segmentation is still a challenging field as it involves 3-D histogram unlike the 1-D histogram of grayscale images. Effectiveness of entropy based multi-level thresholding for color image is yet to be explored and this paper presents a humble contribution in this context. We have used Differential Evolution (DE), a simple yet efficient evolutionary algorithm of current interest, to improve the computation time and robustness of the proposed algorithm. The performance of DE is also investigated extensively through comparison with other well-known nature inspired global optimization techniques like Genetic Algorithm (GA), Particle Swarm Optimization (PSO), and Artificial Bee Colony (ABC). The proposed method is evaluated by comparing it with seven other prminent algorithms both qualitatively and quantitatively using a well known benchmark suite - the Barkley Segmentation Data Set (BSDS300) with 300 distinct images. Such comparison reflects the efficiency of our algorithm.

Keywords:
Multi-Level image segmentation
Color image
Minimum Cross Entropy thresholding
Differential Evolution
Berkeley Segmentation Dataset and Benchmark

1. Introduction

Image segmentation, the process of partitioning an image into meaningful parts or objects, appears as a fundamental step in many image, video, and computer vision related applications. It is a critical step towards content analysis and interpretation of various types of images such as medical images, satellite images, and natural images. For the first two types, gray scale images are the preferred and available source, while for later, the colour images are widely acceptable.

Segmentation obtained through bi-level thresholding subdivides an image into two homogenous regions based on texture, histogram, edge etc. In literature, several image segmentation techniques, such as gray level thresholding, interactive pixel classification, neural network based approaches, edge detection, and fuzzy rule based segmentation have been reported [Fu and Mui, 1981; Pal and Pal, 1993; Sezgin and Sankur, 2004; Sahoo *et al*.,1988; Dey *et al*., 2010; Zhanga *et al.*, 2008.]. Among these methods, gray level global thresholding techniques are the most popular ones and many algorithms have been proposed in this direction, see for example the works of Kapur *et al*. (1985), Wong and Sahoo (1989), Pal (1996), Li and Lee (1993), Otsu (1979) and Rosin (2001).

Entropy-based global thresholding scheme has received considerable attention from the researchers, working on segmentation. The principal assumption of entropy-based global thresholding stands on the entropy of the image histogram as a summation of two regions - the object(s) and the background. Recent developments in information theory have intensified the opportunity to investigate the use of various entropies to find efficient separation between objects and background. Some of these such as Shannon Entropy, Renyi entropy [Sahoo and Arora, 2004], Tsallis entropy [Portes de Albuquerque, 2004], and cross entropy [Li and Tam, 1998] etc. have been widely used for thresholding images. Among the nonparametric approaches cross entropy proposed by [Kullbak, 1968] is perhaps the most preferable technique. Note that all the above mentioned techniques are for bi-level thresholding. A more practical approach for image thresholding is to consider multiple levels so that the image may be divided into more than one objects and background. However the main problem associated with multi-level thresholding is its large time complexity [Kittler and Illingworth, 1986; Pun, 1981; Wang *et al.*, 2008; Zahara *et al.*, 2005]. Researchers used various methods to enhance the computational speed of multi-level thresholding based approaches see for example [Yu *et al.*, 2008; Dirami *et al.*, 2013; Arora *et al.*, 2008; Sezgin and Taşaltín, 2000; Yin and Chen, 1997]. Formulating total entropy as an objective function and solving it by using global optimization algorithms attracted considerable attention in recent years [Hammouche *et al*., 2010].

Metaheuristics provide a very popular way to yield near optimal solutions of a wide variety of complex optimization problems without requiring the knowledge of derivatives or without being sensitive to the choice of initial solutions. Derivative-free metaheuristic optimizers, based on the simulations of some natural phenomena, have been widely used for segmenting images through both bi-level and multi-level thresholding, see for example [Akay, 2013; Marciniak *et al.*,2014; Tao *et al*., 2003; Bazi *et al*., 2007; Hammouche *et al*., 2008]. Applications of some well-known metaheuristics like Genetic Algorithms (GAs) [Tang *et al.*, 2011], Particle Swarm Optimization (PSO) [Akay, 2013; Sathya and Kayalvizhi, 2010; Yin, 2007], Artificial Bee Colony (ABC) [Xiao *et al.*, 2007] etc. can also be found in literature on segmentation and thresholding. Differential Evolution (DE) is arguably one of the most powerful as well as popular evolutionary real-parameter optimizers of current interest [Storn and Price, 1997; Das and Suganthan, 2011]. It has been shown that DE can outperform state-of-art metaheuristics like GA and PSO when it is used for multi-level thresholding based image segmentation [Sarkar *et al*., 2011, 2012; Sarkar and Das, 2013]. However, all the above mentioned algorithms were tested on grayscale images. For segmentation of practical interest a color image is more acceptable than the gray scale images.

Color image segmentation involves subdividing an image into homogeneous regions based on the color information, texture, and edges. However, unsupervised natural color image segmentation still remains a challenge for the researchers. Several works have been published in the last two decades in this direction. Some of the well cited techniques are mean-shift clustering [Comaniciu and Meer, 2002; Luo and Khoshgoftaar, 2006], graph based methods [Shi and Malik, 2000; Felzenszwalb and Huttenlocher, 2004], region based split and merge techniques [Vincent and Soille, 1991; Garcia Ugarriza *et al.,* 2009], Markov random field models [Mignotte, 2010], histogram based method [Cheng *et al.*, 2002], Hybrid methods [Chen *et al.*, 2010; Siang Tan and Mat Isa, 2011], texture based color image segmentation [Krinidis and Pitas, 2009] , pixel clustering [Yu *et al.*, 2010] , principal component analysis based method [Han *et al.*, 2013] etc. The entropy based methods are yet to be applied on color images for achieving natural segmentation.

In this work, we propose an automatic multi-level color image thresholding scheme based on the Minimum Cross Entropy Thresholding (MCET) computationally aided with the DE algorithm. DE is used to reduce the computational time for optimization while still maintaining sufficient accuracy. Extensive simulations have been undertaken to demonstrate the efficiency and robustness of the DE based scheme in comparison to three other popular nature-inspired optimization techniques: GA, PSO, and ABC. An extensive comparative study is also presented on the 300 images from the Berkeley Segmentation Data Set (BSDS 300) involving seven no-evolutionary segmentation methods and on the basis of the performance metrics like Probability Rand Index (PRI), Variation of Information (VOI), Global Consistency Error (GCE), and Boundary Displacement Error (BDE) in context to multilevel thresholding. The outcomes of the DE-based MCET segmentation is tested for different number of threshold levels and assessed by using human made segmentations on the basis of the aforementioned performance metrics. The experimental results reported in this study are also compared with some widely popular color image segmentation schemes.

The paper is organized in the following way. Section 2 briefly introduces the cross entropy and multi-level minimum cross entropy along with their mathematical formulations. The DE algorithm is outlined in Section 3. Section 4 describes the proposed approach in sufficient details. Experimental results of applying the proposed method to the BSDS 300 benchmarks along with statistical analyses and comparison with other metaheuristics and segmentation algorithms have been provided in Section 5. Finally the paper is concluded in Section 6.

2. Minimum Cross Entropy Thresholding (MCET)

2.1. *Cross Entropy*

Let $F = \{f_1, f_2, \dots, f_N\}$ and $G = \{g_1, g_2, \dots, g_N\}$ be two probability distributions on the same set. The cross entropy between F and G is defined by [Kullbak, 1968]:

$$D(F,G) = \sum_{i=1}^{N} f_i \, log \frac{f_i}{g_i}. \quad (1)$$

In order to understand the concept of multilevel thresholding of color images, we briefly overview the bi-level thresholding for color images. The performance of the segmentation algorithm is partially dependent on the choice of color spaces due to non uniform illumination of regions. Literature reveals that perceptually uniform spaces like $L^*a^*b^*$ or $L^*u^*v^*$ achieves significantly better outcomes for segmentation problems than non-uniform color space like *RGB* [Paschos, 2001], which was designed for better representation of color. As an initial step of our algorithm we have converted all the *RGB* images to CIE $L^*a^*b^*$ color space using MATLAB, which creates three components L^*, a^*, and b^*. "L^*" indicates lightness whereas "a^*" and "b^*" represent colors, precisely "a^*" for red-green and "b^*" for blue-yellow. All the component values are between 0 and 255 (8-bit color images).

Let I be an original color image and $h(i)$ be the histogram of the corresponding image which is calculated by combining three components to preserve the color information i.e. $h(i) = (L^*_i; a^*_i; b^*_i)$ for $i = 1,2,.., L$ where L^*_i, a^*_i and b^*_i represent i^{th} intensity value of the channels, L indicating the number of gray levels, i.e. 256. Then the thresholded image I_t can be expressed as:

$$I_t(x,y) = \begin{cases} \mu(1,t) & I(x,y) < t, \\ \mu(t, L+1) & I(x,y) \geq t, \end{cases} \quad (2)$$

where t denotes the selected threshold which divides the image into two regions (object and background) and $\mu(a,b) = \sum_{i=0}^{b-1} ih(i) / \sum_{i=0}^{b-1} h(i)$. The cross entropy is then calculated as proposed by Li and Lee (1993):

$$D(t) = -\sum_{i=1}^{t-1} ih(i) \log\left(\frac{i}{\mu(1,t)}\right) + \sum_{i=t}^{L} ih(i) \log\left(\frac{i}{\mu(t,L+1)}\right) \quad (3)$$

The MCET determines the optimal threshold t^* by minimizing the cross entropy:

$$t^* = \arg\min_t D(t) \quad (4)$$

The computational complexity for determining t^* is $O(nL^2)$. However, the computational complexity tends to be very high for multilevel thresholding, where for n threshold values it jumps to $O(nL^{n+1})$ [Tang *et al.*, 2011].

2.2. *Recursive MCET*

The MCET objective function of eqn. (4) can be rewritten as [Hammouche *et al.*, 2008; Yin, 2007]:

$$D(t) = -\sum_{i=1}^{L} ih(i) \log(i) - \sum_{i=1}^{t-1} ih(i) \log(\mu(1,t)) - \sum_{i=t}^{L} ih(i) \log(\mu(t, L+1)). \quad (5)$$

Since the first term is constant for a given image, the objective function can be redefined as:

$$\begin{aligned}\delta(t) &= -\sum_{i=1}^{t-1} ih(i) \log(\mu(1,t)) - \sum_{i=t}^{L} ih(i) \log(\mu(t,L+1)) \\ &= -\left(\sum_{i=1}^{t-1} ih(i)\right) \log\left(\frac{\sum_{i=1}^{t-1} ih(i)}{\sum_{i=1}^{t-1} h(i)}\right) - \left(\sum_{i=t}^{L} ih(i)\right) \log\left(\frac{\sum_{i=t}^{L} ih(i)}{\sum_{i=t}^{L} h(i)}\right) \\ &= -m^1(1,t) \log\left(\frac{m^1(1,t)}{m^0(1,t)}\right) - m^1(t,L+1) \log\left(\frac{m^1(t,L+1)}{m^0(t,L+1)}\right), \end{aligned} \quad (6)$$

where $m^0(a,b) = \sum_{i=1}^{b-1} h(i)$ and $m^1(a,b) = \sum_{i=1}^{b-1} ih(i)$ are the zero-moment and first-moment on partial range of the image histogram. The recursive programming technique can be easily applied to multilevel thresholding. Assume n is the number of selected thresholds denoted by $t_1, t_2, t_3 \dots\ t_n$. For the convenience of the illustration two dummy thresholds $t_0 \equiv 0$, $t_{n+1} \equiv L+1$ along with $t_0 < t_1 < \dots < t_n < t_{n+1}$ can be added. The objective function for multi-level thresholding then becomes:

$$\delta(t_1, t_2, \dots\dots, t_n) = m^1(t_{i-1}, t_i) \log\left(\frac{m^1(t_{i-1}, t_i)}{m^0(t_{i-1}, t_i)}\right). \quad (7)$$

It is found that the complexity of computing the right hand side of (7) is $O(nL^n)$, which is marginally lesser than $O(nL^{n+1})$ [Tang *et al.*, 2011] but still remains computationally expensive. To reduce the complexity further, we have used DE in our approach for minimizing $\delta(t)$. Being an unsupervised technique, the possible value of n, largely depends on the user input. However, inadequate value of n can lead to under-segmentation or over-segmentation problem.

3. Differential Evolution (DE)

The initial generation of a standard DE algorithm [Storn and Price, 1997; Das and Suganthan, 2011] consists of the four basic steps – initialization, mutation, recombination or crossover, and selection, of which, only last three steps are repeated into the subsequent DE generations. The generations continue till some termination criterion (such as exhaustion of maximum functional evaluations) is satisfied.

The i^{th} individual (parameter vector) of the population at generation G is a D-dimensional vector containing a set of D optimization parameters (search variables):

$$\vec{Z}_{i,G} = [z_{i,1,G}, z_{i,2,G}, \dots \dots, z_{i,D,G}]$$

The individuals of the initial population are randomly generated from a uniform distribution within the search-space. The search-space has maximum and minimum bounds in each dimension and the bounds can be expressed as: $\vec{Z}_{\max} = [z_{\max,1}, z_{\max,2}, \dots, z_{\max,D}]$ and $\vec{Z}_{\min} = [z_{\min,1}, z_{\min,2}, \dots, z_{\min,D}]$. The j-th component of the i-th individual is initialized in the following way:

$$z_{i,j}(0) = z_{\min,j} + rand_{i,j}(0,1) \cdot (z_{\max,j} - z_{\min,j}), \quad (8)$$

with $j \in \{1, 2, \dots, D\}$. Here $rand_{i,j}(0,1)$ is a uniformly distributed random number in (0, 1) and it is instantiated independently for each j^{th} component of the i^{th} individual.

In each generation to change a population member $\vec{Z}_{i,G}$ (say), a corresponding *donor* or mutant vector $\vec{Y}_{i,G}$ is created. It is the method of creating this donor vector that distinguishes the various DE schemes. In one of the earliest variants of DE, now called DE/rand/1 scheme, to create $\vec{Y}_{i,G}$ for each i^{th} member, three other parameter vectors (say the r_1, r_2, and r_3-th vectors such that $r_1, r_2, r_3 \in [1, Np]$, *Np* denoting the population size, and $r_1 \neq r_2 \neq r_3$) are chosen at random from the current population. The donor vector $\vec{Y}_{i,G}$ is then obtained by perturbing any one of the three with a scaled difference of the other two vectors. The process of *mutation* for the j^{th} component of the i^{th} vector may be expressed as,

$$y_{i,j,G} = z_{r1,j,G} + F.(z_{r2,j,G} - z_{r3,j,G}), \quad (9)$$

where F is a scalar number (called the scale factor of DE and usually in [0.4, 2]) controlling the amplification of the difference vector.

Next a *crossover* operation takes place. The DE family of algorithms can use two kinds of crossover schemes - *exponential* (or two-point modulo) and *binomial* (or uniform) [Storn and Price, 1997]. The binomial crossover scheme is briefly explained below since it is used in the proposed method. The binomial crossover is performed on each of the D variables with a probability determined by the control parameter *Cr*, also called the crossover rate for DE. In this case the number of parameters inherited from the mutant has a (nearly) binomial distribution. Thus, corresponding to each target vector $\vec{Z}_{i,G}$, a *trial* vector (the final offspring) $\vec{R}_{i,G}$ is created in the following way:

$$r_{i,j,G} = \begin{cases} y_{i,j,G} & if\ rand_{i,j}(0,1) \leq Cr\ or\ j = rn(i) \\ z_{i,j,G} & otherwise, \end{cases} \quad (10)$$

where j = 1, 2,.., D and $rand_{i,j}(0,1) \in [0,1]$is same as for (1). $rn(i) \in [1, 2, \dots \dots, D]$ is a randomly chosen integer index to ensure that $\vec{R}_{i,G}$ gets at least one component from $\vec{Z}_{i,G}$. Finally '*selection*' is performed to determine which one between the target and the trial vectors will survive to the next generation. If the trial vector yields a better value of the objective function, it replaces its target vector in the next generation; otherwise the parent is retained in the population as:

$$\vec{Z}_{i,G+1} = \begin{cases} \vec{R}_{i,G} & if\ \ f(\vec{R}_{i,G}) \leq f(\vec{Z}_{i,G}) \\ \vec{Z}_{i,G} & if\ \ f(\vec{R}_{i,G}) > f(\vec{Z}_{i,G})' \end{cases} \quad (11)$$

where $f(.)$ is the function to be minimized. Ghosh *et al.* (2012) recently presented a control theoretic proof of convergence of this algorithm under minor regularity assumptions. Fig. 1 shows a block diagram description of the optimization process and also illustrates the link of MCET function with DE.

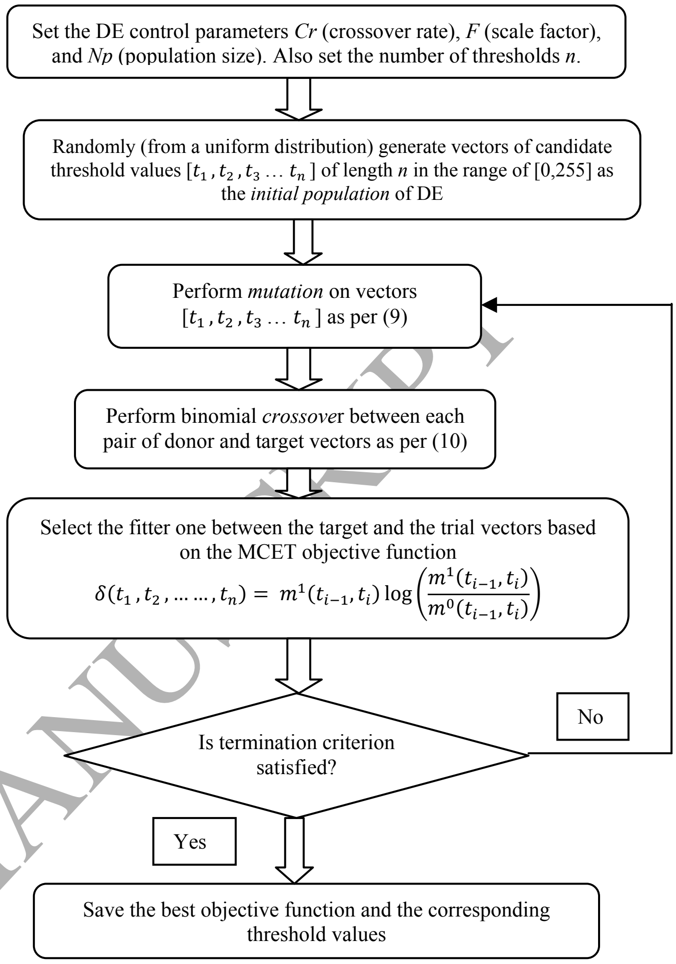

Fig. 1. Flow-chart for the selection of threshold values using DE

4. Color Image Segmentation Based On Multi-Level MCET

In this section we describe the color image segmentation process using the idea of multi-level MCET and DE. The histogram for color images $h(i)$ is calculated and used (as in eqn. (6)) to form the objective function for the DE algorithm. The threshold values are attained by minimizing the objective function and the segmented *RGB* color images are formed with these threshold values. The *RGB* color space is used to demonstrate differences of regions more prominently.

For better discrimination between the different segmented objects, the small regions are needed to be removed or merged into relatively bigger regions. A well known region merging technique called Statistical Region Merging (SRM) [Nock and Nielsen, 2004] is used after obtaining the thresholded image to remove small regions by merging them into larger regions. The amount of merged regions is largely dependent on softness or hardness of the SRM algorithm which is decided by the Q value. Variation of Q allows reduction of the statistical complexity of the scene and in turn controls the coarseness of the segmentation, with the opportunity to establish a hierarchy of coarse-to-fine (multiscale) segmentations of an image. Larger value of Q, results softly merged region and with decrease of Q, the hardness of the merged regions increases. For Q=1, it will be inconvenient to find small homogenous regions. Larger Q values generate larger number of homogenous regions and increase chances of accurate segmentation. In our paper we are using SRM as post processing to remove small regions and the value of Q will work differently here from the traditional SRM method as described in

[Nock and Nielsen, 2004]. A thorough discussion on possible value of Q and its effect on segmenting different regions of a natural image have been provided in Section 5.The entire procedure along with examples of the outputs in different stages is demonstrated in Fig. 2.

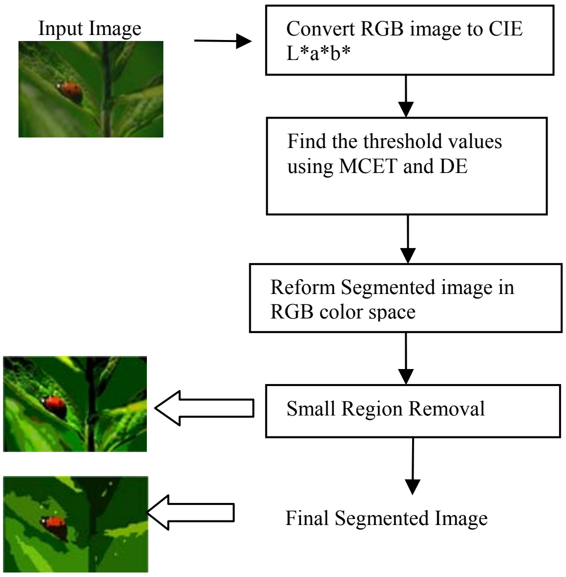

Fig. 2. Block diagram of the proposed algorithm

5. Experimental Results

5.1. Experimental Setup

All the simulations have been performed using MATLAB R2012a in a workstation with Intel® Core™ i3 3.2 GHz processor. The DE/rand/1/bin scheme (it is the DE/rand/1 scheme explained in Section 3 with the binomial crossover) is used to compute the threshold levels efficiently. The parametric settings of DE, GA, PSO, and ABC have been adopted using the guidelines provided in the respective literatures [Hammouche *et al.*, 2010; Sarkar and Das, 2013]. Results have been obtained by replacing DE with these algorithms in the same procedure illustrated in Fig. 1. Results of the metaheuristic algorithms have been provided as the mean of 50 independent runs where each run was continued till the exhaustion of $D\times1000$ number of Function Evaluations (FEs), D denoting the search space dimensionality. To make the comparison fair enough, instead of number of generations/iterations, we continued each run of each algorithm till the same number of FEs. This is because of the fact that in evolutionary computing community, number of FEs is a reliable measure for computation time as different algorithms may perform different amounts of works in their inner loops. Note that for an Lv levels segmentation problem the dimensionality of the search space is $D = Lv$-1. The number of segmented level (Lv) considered for experiment are 5, 7, and 10. As the numbers of actual segments are unknown, we presented an approach to avoid the under-segmentation/over-segmentation problem by selecting higher values of n along with SRM to remove region small regions.

To measure the performance of the proposed technique from image segmentation perspective, four performance indices [Unnikrishnan *et al.*, 2007] were used. The details of these indices are presented in Section 5.2. The MATLAB code of the indices along with the benchmark images can be obtained from http://www.eecs.berkeley.edu/~yang/software/lossy_segmentation/SegmentationBenchmark.zip. For performance measurements, the finally segmented RGB images are converted into label matrix for quantitative comparison with (i.e. labeling the segmented regions) ground truth images.

5.2. Performance Evaluation and Comparison

For testing and analyses, 300 images were used from the Berkeley Segmentation Data Set and Benchmark (BSDS 300). The dimension of each image is 481×321. For each image, a set of benchmark images compiled by the human observers is provided. All the images are normalized to have the longest side equals to 320 pixels [Yang et al., 2006, 2008; Mignotte, 2008]. The following image segmentation indices were used. *Probability Rand Index* (*PRI*), *Variation of Information (VoI*), *Global Consistency Error* (*GCE*): *Boundary Displacement Error* (*BDE)* [Unnikrishnan *et al*., 2005, 2007; Pantofaru and Hebert, 2005; Meila, 2005; Martin *et al*., 2001; Freixenet *et al*., 2002]. These complementary measures have to be considered all together to evaluate the performance of a given segmentation method. *Higher* value of PRI indicates better segmentation, whereas for rest of the indices *lower* values point out the same. The results of DE based MCET (denoted as MCET_DE) are compared with popular color image segmentation methods like Compression based Texture Merging (CTM) [Yang et al., 2008], mean-shift [Comaniciu and Meer, 2002], Normalized cuts (Ncuts) [Shi and Malik, 2000] , Nearest Neighbor Graphs (NNG) [Felzenszwalb and Huttenlocher, 2004] and SCL (post processed) **[**Huang *et al*., 2011**]**. The results for these four algorithms were obtained from [Yang *et al*., 2006, 2008].

Table 1: Performance of DE, PSO, GA (computed over 300 images from BSDS300 set)

Lv	**Algo.**	**Run Time (in Sec.)**	f_{mean}	f_{std}	***P*-Values**
5	DE	**2.5549**	$\mathbf{-2.89342\times10^{08}}$	**40.4902**	**NA**
	PSO	3.0451	-2.89331×10^{08}	7.1364×10^{03}	3.76×10^{-4}
	GA	3.3606	-2.89320×10^{08}	2.4312×10^{03}	5.27×10^{-6}
	ABC	3.1021	-2.89334×10^{08}	3.7605×10^{03}	8.41×10^{-5}
7	DE	**3.1754**	$\mathbf{-2.89428\times10^{08}}$	**21.4823**	**NA**
	PSO	6.5253	-2.89403×10^{08}	7.1140×10^{03}	1.58×10^{-3}
	GA	6.3569	-2.89412×10^{08}	1.7096×10^{03}	5.03×10^{-5}
	ABC	6.4127	-2.89403×10^{08}	3.5181×10^{03}	2.74×10^{-6}
10	DE	**5.5587**	$\mathbf{-2.89464\times10^{08}}$	**44.2000**	**NA**
	PSO	18.4876	-2.89442×10^{08}	3.5503×10^{03}	3.66×10^{-7}
	GA	12.0203	-2.89451×10^{08}	1.7177×10^{03}	2.71×10^{-6}
	ABC	14.7001	-2.89458×10^{08}	1.9824×10^{03}	6.93×10^{-5}

A non-parametric statistical test, called the Wilcoxon's rank sum test for independent samples [Wilcoxon, 1945; Derrac *et al.*, 2011], was conducted at the 5% significance level in order to judge whether the results obtained with the best performing algorithm differ from the final results of rest of the competitors in a statistically significant way. If the *P*-values are less than 0.05 (5% significance level), it is a strong evidence against the null hypothesis, indicating that the better final objective function values achieved by the best algorithm in each case is statistically significant and has not occurred by chance [Derrac *et al.*, 2011]. The average computation time (in sec), average mean objective value (f_{mean}) and standard deviation (f_{std}) computed on 300 color images of the BSDS300 dataset are displayed in Table 1. The best in the class results are marked in bold letters. DE outperformed the other three peer metaheuristics in a statistically meaningful way and it also emerged as the fastest of the algorithms compared. The performance of DE clearly remained very robust as indicated by the significantly less value of the standard deviations in all cases as compared to the standard deviations obtained using GA, PSO, and ABC.

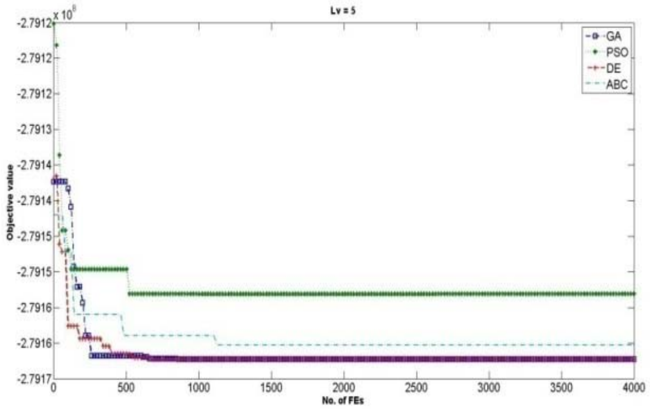

Fig. 3(a). Convergence plot of GA, PSO, DE, and ABC for Lv = 5 for image “100080.jpg” from the BSDS300 set.

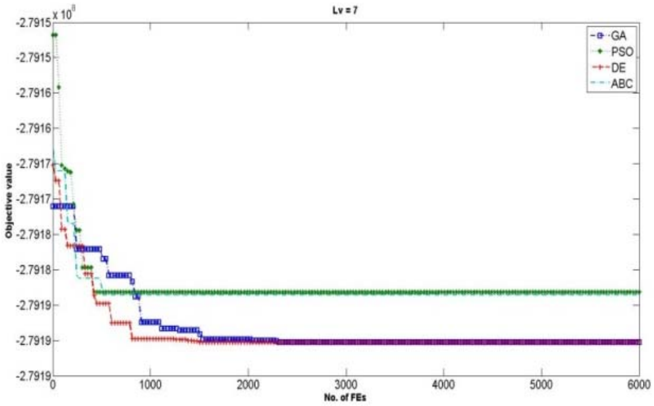

Fig. 3(b). Convergence plot of GA, PSO, DE and ABC for Lv = 7 for image “100080.jpg” from the BSDS300 set.

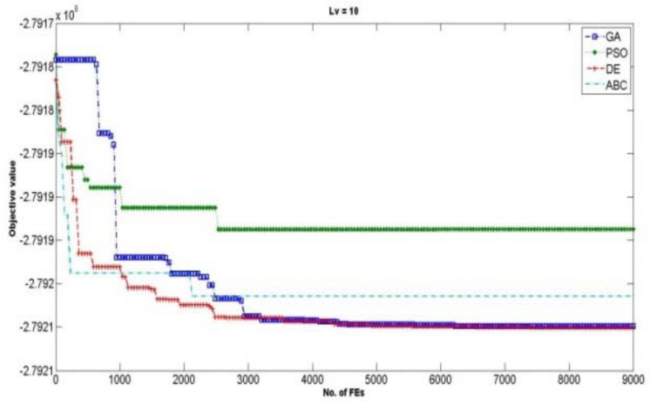

Fig. 3(c). Convergence plot of GA, PSO, DE and ABC for Lv =10 for image “100080.jpg” from the BSDS300 set.

Fig. 3 displays the sample convergence plots of the employed metaheuristic algorithms for Lv = 5 (Fig. 3 (a)), 7 (Fig. 3(b)), and 10 (Fig. 3(c)) on a sample image from the BSDS300 set with identification number 100080. For five levels, DE attains the convergence around after 200 FEs (Fig. 3 (a)). GA closely follows DE. PSO converges faster than ABC (600 FEs in comparison of 1200 FEs for ABC), but PSO shows premature convergence. For 7 levels segmentation (Lv = 7) DE reaches the minimum objective value before 1500 FEs, whereas GA took at least 2200 FEs to achieve the same level (Fig. 3(b)). PSO and ABC converged faster than others but they were also trapped in local minima and resulted in higher objective values as compared to DE. As shown in Fig. 3(c), DE is the fastest among all the algorithms to get to the lowest objective function value (after 4500 FEs) while the others struggle to converge. DE also reports minimum objective value for Lv = 5, 7 and 10. The performance of GA closely follows DE in terms of the minimum objective value, while PSO exhibits the weakest convergence characteristics. The application of metaheuristics is essential for multi-level thresholding and application of DE would certainly strengthen the algorithms by adding speed and robustness.

Table 2: Comparison of average benchmark results for MCET_ DE with other standard algorithms (computed over 300 images from Berkley Image Segmentation Dataset)

Algorithm	BDE	PRI	GCE	VOI
Ground Truth	4.9940	0.8754	0.0797	1.1040
Meanshift	9.7001	0.7550	0.2598	2.4770
Ncuts	9.6038	0.7229	0.2182	2.9329
FH/NNG	9.9497	0.7841	0.1895	2.6647
CTM $_{\eta=0.2}$	9.8962	0.7617	0.1877	2.0236
CTM $_{\eta=0.1}$	9.4211	0.7561	0.1767	2.4640
SCLpost, λ=200	9.8946	0.7506	0.1689	1.9501
MCET_DE$_{Q=15}$ [Lv 5]	9.8161	0.7533	0.2586	2.2761
MCET_DE$_{Q=15}$ [Lv 7]	9.6597	0.7493	0.2542	2.1864
MCET_DE$_{Q=15}$[Lv 10]	9.3468	0.7552	0.2485	2.1675

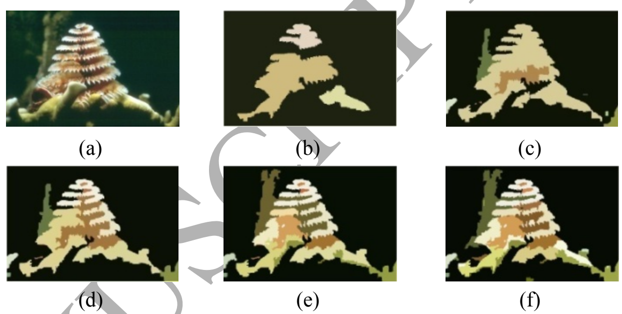

Fig.4. Example of effect of “Q” value on a 5-level segmented image for values (a) original color image(b) 2 (c) 5 (d) 10 (e) 15 (f) 20

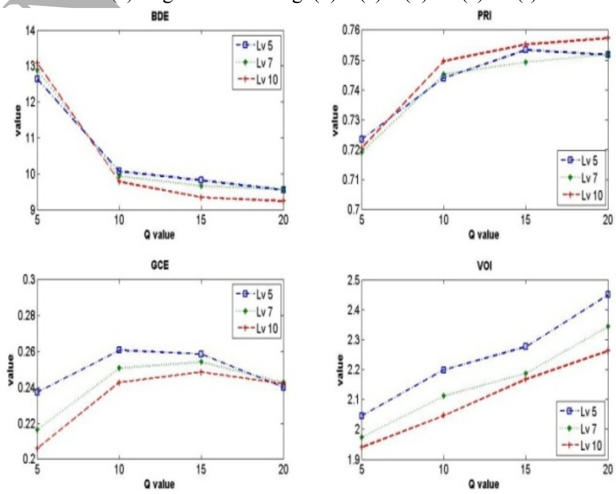

Fig. 5. Demonstration of Changes in outcomes for different Lv for BSD 300 Benchmarks

Statistical Region Merging is used on threholded image to remove small region of less than 10 pixels. However, the performance of SRM predominately depends on softness or hardness of the region merging technique. In this paper we have also examined a possible value of the parameter Q, which is a key factor for deciding the achieved softness or hardness of the merged regions [Nock and Nielsen, 2004], both qualitatively and quantitatively by using BSDS300 dataset and benchmarks. Fig. 4 exhibits the effect of Q value on a 5-level segmented image by varying it from 2 to 20 (Figs. 4(b) – 4(f)). It is clearly noticeable from Fig. 4 that lower Q values result into hard segmented regions i.e. small number of large regions, whereas higher Q values give more number of smaller regions. Although too much soft segmentation would increases the risk of improper region identification. Thus, it is important to set proper balance between soft and hard segmentations by selecting adequate value of the parameter Q. In this work we tried to address this problem of choosing proper value Q for achieving better segmented region by means of performance evolution benchmarks of BSD300 dataset. We have varied Q value from 5 to 20 for Lv=5, 7, and

10 on thresholded image obtained by using MCET along with DE. The average BDE, PRI, GCE, and VOI over 300 images of the dataset are plotted in Fig. 5. The plots reveal betterment of results in terms of VOI and GCE with lower value Q on contrary of the PRI and BDE measurements. VOI measurement for $Q = 5$ even beats the results obtained by CTM, which give best in the results for VOI by quite a margin (VOI for MCET_DE$_{Q=5}$ are as follows: 2.0447 for $Lv = 5$, 1.9727 for $Lv = 7$, and 1.9394 for $Lv = 10$) but at the same time PRI and BDE are not even closer to the standard results (BDE and PRI for $Lv = 5$, 7, and 10 are over 12.5 and under 0.71 respectively, whereas as reported in Table 6 the lowest value of BDE and PRI reported in standard algorithms are 9.9497 and 0.7229 respectively). A careful study of the results reported in Fig. 5 reveals that at $Q = 15$, all the performance evolution metrics give well balance results. Hence, we suggest a value of $Q = 15$ for SRM algorithm to achieve better segmented results after thresholding by MCET_DE algorithm.

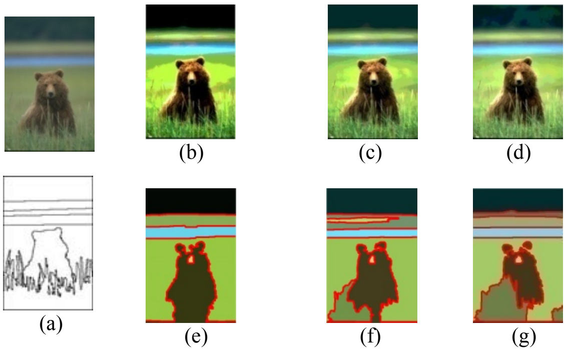

Fig. 6. Example of MCET_DE on image "100080.jpg": (a) Original color image and its ground truth (b) 5 *Lv* segmented image for threshold values [78,106,125,139] , (c) 7 *Lv* segmented image for threshold values [56,81,107,123,133,144], (d) 10 *Lv* segmented image for threshold values [52,65,76,94,111,122,130,139,147] ; After Region Merging (e) 5 *Lv* , (f) 7 *Lv*, (g) 10 *Lv*.

The outcomes of DE based MCET for $Q = 15$ (MCET_DE$_{Q=15}$) for $Lv = 5$, 7, and 10 are showed in Table 2 along with ground truth results (i.e. ideal) and other popular color image segmentation methods. MCET_DE$_{Q=15}$ attained best in the class measurement for BDE at $Lv = 10$. Also MCET_DE$_{Q=15}$ reports 2nd best results for VOI after CTM$_{\eta=0.2}$ and SCL at all levels. The PRI values are not best in the class (The best result attained by FH/NNG) but pretty much comparable with CTM, SCL and Meanshift techniques. Only shortcoming of the MCET_DE$_{Q=15}$ is perhaps the GCE outcomes, which is lesser than all the algorithms except Meanshift.

The acquired threshold values for 3, 5, and 7 level segmentations and the resulting images by using MCET and DE based techniques are illustrated via some examples from the BSDS300 dataset in Figures 6 and 7. The qualitative comparisons of segmented outputs with existing methods and ground truth images from BSD300 dataset are displayed in Fig. 7. For image "198004.jpg" only MCET_DE, CTM and SCL gives results close to its ground truth images, while others fails to deliver the expected outcome. MCET_DE, CTM and SCL outperformed other approaches in image "23025.jpg". Fig. 7 clearly shows that the outcomes of our methodology remain sufficiently close to the ground truth images and in various occasions outperforms the existing approaches. Only results of CTM and SCL are comparable with outcomes of MCET_DE. The qualitative comparison displayed in Fig. 7 supports the quantitative comparison of different methods as displayed in Table 2.

6. Conclusion

A histogram based natural color image segmentation technique by using multi-level minimum cross entropy and an evolutionary algorithm (DE) is proposed. MCET based approach aided with DE delivers acceptable results in reasonable amount of computational time. DE has been shown to outperform three widely known derivative-free metaheuristic global optimizers GA, PSO, and ABC. A popular region merging technique called statistical region merging is applied along with MCET to obtain more distinguishable regions. The improvement in segmentation using DE and SRM is established via performance evaluation indices and color images from the Berkley image segmentation dataset BSDS300. Finding the right value of Q is crucial for the deciding regions in SRM technique. It is evident from the experiments undertaken in our work that a balanced result in terms of softness or hardness of the region boundary can be obtained for $Q = 15$ without affecting the outcomes much. In future, adaptive image dependent method and multi-objective optimization procedure may be investigated in this context. Also fuzzy entropy can be used for the histogram based color image segmentation in order to achieve better results in multi-level thresholding. More efficient and sophisticated region merging techniques can also be integrated with multi-level thresholding to remove small regions and to accomplish more defined regions.

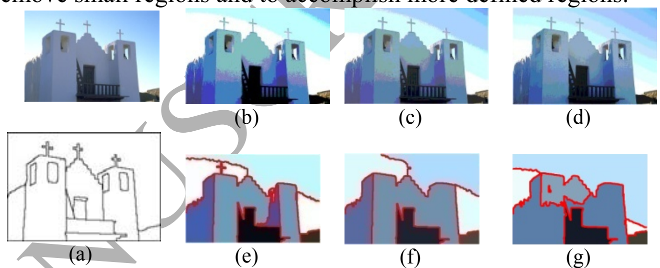

Fig. 7. Example of MCET_DE on image "24063.jpg": (a) Original color image and its ground truth (b) 5 *Lv* segmented image for threshold values [72,117,136,183], (c) 7 *Lv* segmented image for threshold values [37,78,117,135,173,220] (d) 10 *Lv* segmented image for threshold values [36,72,102,115,125,138,169,206,232] ; After Region Merging (e) 5 *Lv* , (f) 7 *Lv*, (g) 10 *Lv*.

References

Akay, B., 2013. A study on particle swarm optimization and artificial bee colony algorithms for multilevel thresholding. *Applied Soft Computing*. 13(6), 3066-3091.

Arora, S., Acharya, J., Verma, A., Panigrahi, B. K., 2008. Multilevel thresholding for image segmentation through a fast statistical recursive algorithm. *Pattern Recognition Letters*. 29(2), 119-125.

Bazi, Y., Bruzzone, L., & Melgani, F., 2007. Image thresholding based on the EM algorithm and the generalized Gaussian distribution. *Pattern Recognition*. 40(2), 619-634.

Chen, S., Cao, L., Wang, Y., Liu, J., Tang, X., 2010. Image segmentation by MAP-ML estimations. *IEEE Transactions on Image Processing,*. *19*(9), 2254-2264.

Cheng, H. D., Jiang, X. H., Wang, J., 2002. Color image segmentation based on homogram thresholding and region merging. *Pattern Recognition*, 35(2), 373-393.

Comaniciu, D., Meer, P., 2002. Mean shift: A robust approach toward feature space analysis. *IEEE Trans. Pattern Anal. Mach. Intell.* 24(5), 603–619.

Das, S., Suganthan, P. N., 2011. Differential evolution: A survey of the state-of-the-art. *IEEE Transactions on Evolutionary Computation,* 15(1), 4-31.

Derrac, J., García, S., Molina, D., Herrera F., 2011. A practical tutorial on the use of nonparametric statistical tests as a methodology for comparing evolutionary and swarm intelligence algorithms. *Swarm and Evolutionary Computation*, 1(1), 3-18.

Dey, V., Zhang, Y., Zhong, M., 2010. A review on image segmentation techniques with remote sensing perspective, In: W. Wagner and B. Székely, (Eds.): ISPRS TC VII Symposium – 100 Years ISPRS. Vienna, Austria.

Dirami, A., Hammouche, K., Diaf, M., Siarry, P., 2013. Fast multilevel thresholding for image segmentation through a multiphase level set method. *Signal Processing*. 93(1), 139–153.

Fu, K.S., Mui, J.K., 1981. A survey on image segmentation. *Pattern Recognition*. 13, 3-16.

Felzenszwalb, P. F., Huttenlocher, D. P., 2004. Efficient graph-based image segmentation. *International Journal of Computer Vision*. 59(2), 167-181.

Freixenet, J., Munoz, X., Raba, D., Marti, J., Cuff, X., 2002, Yet another survey on image segmentation, *Proceedings of European Conference on Computer Vision*. 408–422.

Garcia Ugarriza, L., Saber, E., Vantaram, S. R., Amuso, V., Shaw, M., Bhaskar, R., 2009. Automatic image segmentation by dynamic region growth and multiresolution merging, *IEEE Transactions on Image Processing, 18*(10), 2275-2288.

Ghosh, S., Das, S., Vasilakos, A. V., Suresh, K., 2012. On convergence of differential evolution over a class of continuous functions with unique global optimum. *IEEE Transactions on Systems, Man, and Cybernetics, Part B: Cybernetics,* 42(1), 107-124.

Hammouche, K., Diaf, M., & Siarry, P., 2008. A multilevel automatic thresholding method based on a genetic algorithm for a fast image segmentation. *Computer Vision and Image Understanding*. 109(2), 163-175.

Hammouche, K., Diaf, M., Siarry, P., 2010. A comparative study of various meta-heuristic techniques applied to the multilevel thresholding problem. *Engineering Applications of Artificial Intelligence*. 23(5), 676-688.

Han, Y., Feng, X. C., Baciu, G., 2013. Variational and PCA based natural image segmentation. *Pattern Recognition*. 46(7), 1971-1984.

Huang, R., Sang, N., Luo, D., Tang, Q., 2011. Image segmentation via coherent clustering in L*a*b* color space. *Pattern Recognition Letters,* 32(7), 891–902.

Kapur, J. N., Sahoo, P. K., Wong, A. K. C., 1985. A new method for gray-level picture thresholding using the entropy of the histogram. *Comput. Vision Graphics Image Process*. 29, 273–285.

Kittler, J., Illingworth, J., 1986. Minimum error thresholding. *Pattern Recognition*. 19, 41–47.

Krinidis, M., Pitas, I., 2009. Color texture segmentation based on the modal energy of deformable surfaces. *IEEE Transactions on Image Processing,*. 18(7), 1613-1622.

Kullback, S.,1968. *Information Theory and Statistics*. Dover, New York.

Li, C. H., Lee, C. K., 1993. Minimum cross entropy thresholding. *Pattern Recognition*. 26, 617–625.

Li, C. H., Tam, P. K. S., 1998. An iterative algorithm for minimum cross entropy thresholding. *Pattern Recognition Letters*. 19, 771–776.

Luo, Q., Khoshgoftaar, T. M., 2006. Unsupervised multiscale color image segmentation based on MDL principle. *IEEE Transactions on Image Processing*. *15*(9), 2755-2761.

Martin, D., Fowlkes, C., Tal, D., Malik, J., 2001. A database of human segmented natural images and its application to evaluating segmentation algorithms and measuring ecological statistics. *Proceedings of IEEE International Conference on Computer Vision*. 416– 423.

Marciniak, A., Kowal, M., Filipczuk, P., Korbicz, J. , 2014. Swarm Intelligence Algorithms for Multi-level Image Thresholding. In *Intelligent Systems in Technical and Medical Diagnostics*. Springer Berlin Heidelberg. 301-311.

Meila, M., 2005. Comparing clusterings: an axiomatic view, Proceedings of the International Conference on Machine Learning. 577–584.

Mignotte, M., 2008. Segmentation by fusion of histogram-based-means clusters in different color spaces. *IEEE Transactions on Image Processing*. 17(5), 780-787.

Mignotte, M., 2010. A label field fusion Bayesian model and its penalized maximum rand estimator for image segmentation. *IEEE Transactions on Image Processing*. 19(6), 1610-1624.

Nock, R., Nielsen, F., 2004. Statistical region merging. *Pattern Analysis and Machine Intelligence, IEEE Transactions on*. 26(11), 1452-1458.

Otsu, N., 1979. A threshold selection method for grey level histograms. *IEEE Transactions on System, Man and Cybernetics*. 9(1), 62–66.

Pantofaru, C., Hebert, M., 2005. A comparison of image segmentation algorithms. *Robotics Institute*, carnegie mellon university . 336.

Pal, N. R., Pal, S. K., 1993. A review on image segmentation techniques. *Pattern Recognition*. 26(9), 1277-1294.

Pal, N. R., 1996. On minimum cross entropy thresholding. *Pattern Recognition*. 29(4), 575-580.

Paschos, G., 2001. Perceptually uniform color spaces for color texture analysis: an empirical evaluation. *IEEE Transactions on Image Processing*. 10(6), 932-937.

Portes de Albuquerque, M., Esquef, I. A., Mello, A. R. G.,2004. Image thresholding using Tsallis entropy. *Pattern Recognition Letters*. 25, 1059–1106.

Pun, T., 1981. Entropy thresholding: a new approach. *Computer Vision Graphics and Image Processing*. 16, 210–239.

Rosin, P. L., 2001. Unimodal thresholding. *Pattern Recognition*. 34, 2083–2096.

Sahoo, P. K., Soltani,S. A., Wong, K. C., Chen,Y. C., 1988. A survey of thresholding techniques. *Computer Vision, Graphics, and Image Processing*, 41(2), 233-260.

Sahoo, P. K., Arora, G., 2004. A thresholding method based on two dimensional Renyi's entropy. *Pattern Recognition*. 37, 1149–1161.

Sarkar, S., Patra, G. R., Das, S., 2011. A differential evolution based approach for multilevel image segmentation using minimum cross entropy thresholding. *Swarm, Evolutionary, and Memetic Computing Conference*. LNCS. 7076, 51-58.

Sarkar, S., Chaudhuri, S. S., Das, S., 2012. Multilevel image thresholding based on Tsallis entropy and differential evolution. *Swarm, Evolutionary, and Memetic Computing. Springer Berlin Heidelberg*. LNCS. 7677, 17-24.

Sarkar, S., Das, S., 2013. Multilevel image thresholding based on 2D histogram and maximum Tsallis entropy— a Differential Evolution approach. *IEEE Trans. Image Processing*. 22 (12), 4788 – 4797.

Sathya, P. D., Kayalvizhi, R., 2010. PSO-based Tsallis thresholding selection procedure for image segmentation. *International Journal of Computer Applications*, 5(4), 39 – 46.

Sezgin, M., Taşaltín, R. , 2000. A new dichotomization technique to multilevel thresholding devoted to inspection applications. *Pattern Recognition Letters*. 21(2), 151-161.

Sezgin, M., Sankur, B., 2004. Survey over image thresholding techniques and quantitative performance evaluation. *Journal of Electronic Imaging*. 13(1), 146–165.

Shi, J., Malik, J., 2000. Normalized cuts and image segmentation. *IEEE Transactions on Pattern Analysis and Machine Intelligence*. 22(8), 888-905.

Siang Tan, K., Mat Isa, N. A., 2011. Color image segmentation using histogram thresholding–Fuzzy C-means hybrid approach. *Pattern Recognition*. *44*(1), 1-15.

Storn, R., Price, K., 1997. Differential evolution - a simple and efficient heuristic for global optimization over continuous spaces. *Journal of Global Optimization*. 11, 341–359.

Tang, K., Yuan, X., Sun, T., Yang, J., & Gao, S., 2011. An improved scheme for minimum cross entropy threshold selection based on genetic algorithm.*Knowledge-Based Systems*. *24*(8), 1131-1138.

Tao, W. B., Tian, J. W., & Liu, J., 2003. Image segmentation by three-level thresholding based on maximum fuzzy entropy and genetic algorithm. *Pattern Recognition Letters*. *24*(16), 3069-3078.

Unnikrishnan, R., Pantofaru, C., Hebert, M., 2005, June. A measure for objective evaluation of image segmentation algorithms. In *Computer Vision and Pattern Recognition-Workshops, 2005. CVPR Workshops. IEEE Computer Society Conference on* . 34-34. IEEE.

Unnikrishnan, R., Pantofaru, C., Hebert, M., 2007. Toward objective evaluation of image segmentation algorithms. *IEEE transactions on Pattern Analysis and Machine Intelligence*. *29*(6), 929-944.

Vincent, L., Soille, P., 1991. Watersheds in digital spaces: an efficient algorithm based on immersion simulations. *IEEE transactions on Pattern Analysis and Machine Intelligence. 13*(6), 583-598.

Wang, S., Chung, F. L., Xiong, F., 2008 . A novel image thresholding method based on Parzen window estimate. *Pattern Recognition*. .41, 117–129.

Wilcoxon, F., 1945. Individual comparisons by ranking methods, *Biometrics*. 1, 80-83.

Wong, A. K. C., Sahoo, P. K., 1989. A gray-level threshold selection method based on maximum entropy principle. *IEEE Trans. Systems, Man and Cybernetics.* 19, 866–871.

Xiao, Y., Cao, Y., Yu, W., & Tian, J., 2012. Multi–level threshold selection based on artificial bee colony algorithm and maximum entropy for image segmentation. *International Journal of Computer Applications in Technology*. 43(4), 343-350.

Yang, A. Y., Wright, J., Ma, Y., Sastry, S. S., 2006. Unsupervised segmentation of natural images via lossy data compression. Elect. Eng. Comput. Sci. Dept. Univ. California, Berkeley. [Online].Available: http://www.eecs.berkeley.edu/Pubs/TechRpts/2006/EECS-2006-95.html

Yang, A. Y., Wright, J., Ma, Y., Sastry, S. S., 2008. Unsupervised segmentation of natural images via lossy data compression. *Computer Vision and Image Understanding*. 110(2), 212-225.

Yin, P. Y., Chen, L. H., 1997. A fast iterative scheme for multilevel thresholding methods. *Signal Processing*, 60(3), 305-313.

Yin, P. Y., 2007. Multilevel minimum cross entropy threshold selection based on particle swarm optimization. *Applied Mathematics and Computation*. *184*(2), 503-513.

Yu, L., Dong, G., Ogunbona, P., Li, W., 2008. An efficient iterative optimization algorithm for image thresholding. *Pattern Recognition Letters*. Vol. 29, 1311–1316.

Yu, Z., Au, O. C., Zou, R., Yu, W., Tian, J., 2010. An adaptive unsupervised approach toward pixel clustering and color image segmentation. *Pattern Recognition*. 43(5), 1889-1906.

Zahara, E., Fan, S. K. S., Tsai, D. M., 2005. Optimal multi-thresholding using a hybrid optimization approach. *Pattern Recognition Letters*. 26, 1082–1095.

Zhanga, H., Frittsb, J. E., Goldmana, S. A., 2008. Image segmentation evaluation: A survey of unsupervised methods. *Computer Vision and Image Understanding*. 110(2), 260–280.

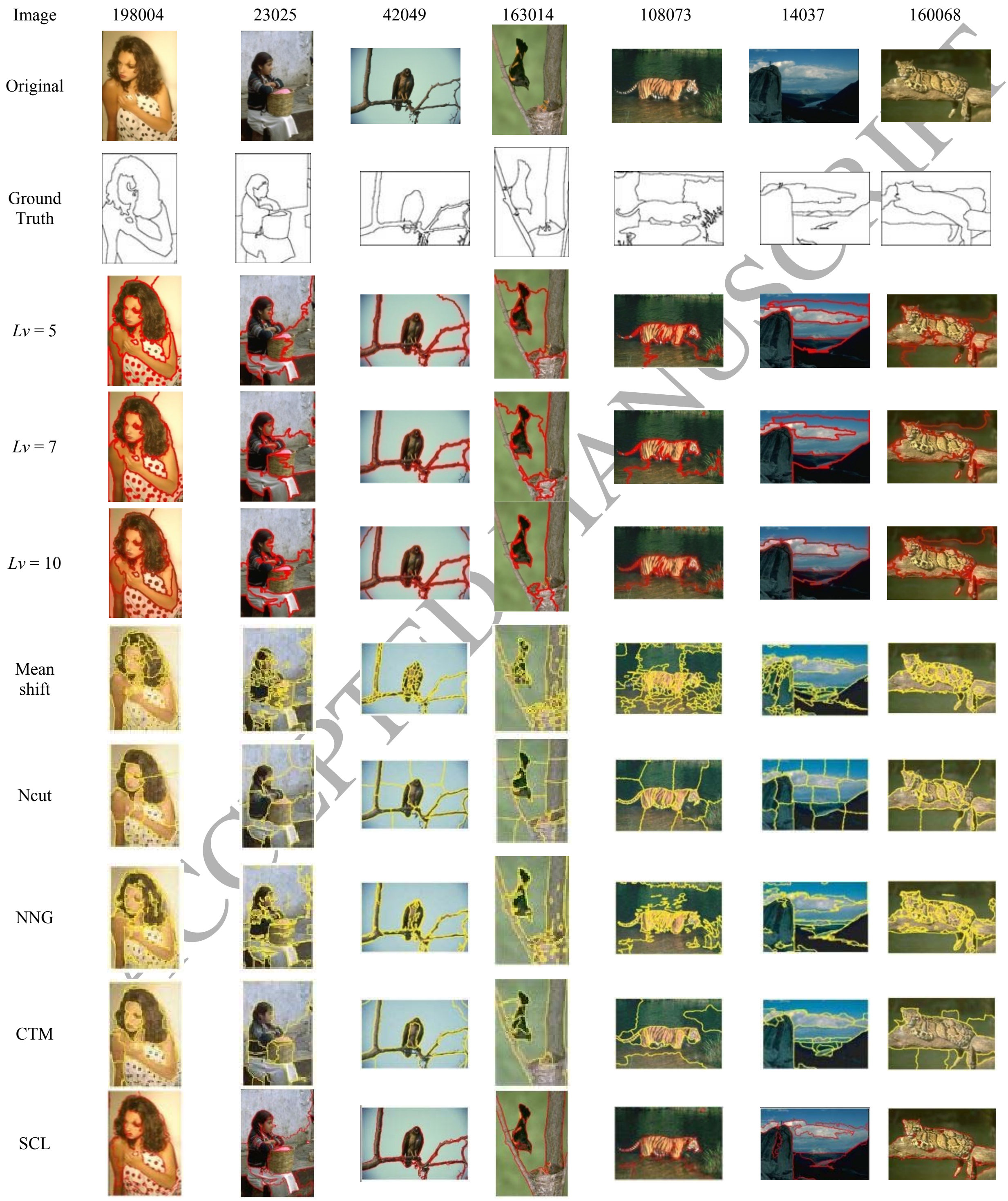

Fig. 8. Qualitative comparison of proposed method with other existing method as found in [Chen *et al.*, 2010, Huang *et al.*, 2011]